Continuous Inverse Class-F GaN Power Amplifier with 70% Efficiency over 1.4-2 GHz Bandwidth

Continuous Inverse Class-F GaN Power Amplifier with 70% Efficiency over 1.4-2 GHz Bandwidth

Anna Piacibello[1], Zhifan Zhang[2], Vittorio Camarchia[3]
Politecnico di Torino, Italy
{[1]anna.piacibello, [3]vittorio.camarchia}@polito.it

***Abstract* — This work presents the design and experimental characterization of a wideband continuous inverse class-F power amplifier, covering several bands in the 5G FR1 frequency range, and thus suitable for base station applications. The design spaces of the class-F and inverse class-F in terms of input and output terminations are reviewed and compared, and the design choices relative to an implementation using a packaged device are described. Measurements show a saturated output power of 40 dBm, with corresponding efficiency and gain higher than 70% and 13 dB, respectively, over 1.4-2 GHz. The performance is well in line with the state of the art and is accurately predicted by simulations, proving the effectiveness of the design strategy.**

***Keywords* — harmonic tuning, power amplifiers, high efficiency, broadband, 5G, base station.**

I. Introduction

Wideband high-efficiency power amplifiers (PAs) able to cover multiple frequency bands are highly desirable for communication systems, both in terms of simplicity of the architecture and cost. However, a trade-off between performance of the PA in terms of power, efficiency, linearity, and operating bandwidth is often required, with a critical effect on the performance of the overall transmitter. In fact, the efficiency of the PA is a key parameter of the communication link, with a strong impact on power dissipation and thus either battery life or the size of the heat sinks.

Despite recent interest shifting towards back-off efficiency enhancement PA architectures, supply modulation, or load modulation [1], the harmonic tuning PAs such as class-F and its derivatives are still being explored for sub-6 GHz applications, such as base stations and tactical ground and air communications, typically targeting output powers in the range 10-100 W. One of the critical requirements in these applications is the PA linearity at the 3 dB gain compression point. If it is high enough, the very high efficiency attainable at saturation makes such PAs competitive also in back-off, and thus suitable for the present scenario. This trend is confirmed by recent examples of PAs based on harmonic tuning, which demonstrate excellent performance both in terms of peak efficiency and relative bandwidth [2], [3].

In this paper we present a continuous inverse class-F power amplifier designed to cover multiple FR1 5G individual radio frequency bands (from 1.4 GHz to 2 GHz), targeting medium-power base station applications. The realized prototype achieves a saturated output power in excess of 40 dBm, with corresponding efficiency and gain higher than 70% and 10 dB, respectively, over the frequency band 1.4-2 GHz (relative bandwidth $>35\%$). The performance is well in line with the state of the art at similar frequencies and is accurately predicted by simulations, proving the effectiveness of the design strategy.

II. Theory Review

Harmonic-tuned PAs could ideally reach 100% efficiency if an infinite number of harmonics could be controlled, and several device non-ideal effects were negligible.

The number of harmonics to be controlled is often a trade-off between the complexity of the matching networks and the cutoff frequency of the adopted active device which, in turn, is deeply affected by the presence or absence of a package. In this work, the selected transistor is the Wolfspeed's 10 W packaged device (CGH40010F), which is suitable for applications up to 6 GHz. As a consequence, targeting the 5G frequency bands up to 2 GHz, the harmonic tuning on the active device is only feasible up to the third harmonic.

According to [4], controlling up to the third harmonic in class-F PAs and their derivatives allows to achieve around 82% drain efficiency. Furthermore, it has been demonstrated that, in practical implementations, inverse class-F PAs can achieve higher efficiency with respect to their class-F counterparts due to a lower effect of the knee voltage, at least in single-frequency designs [5]. However, the continuous class-F and inverse class-F modes have optimum terminations loci with opposite rotation directions on the Smith chart, which could result in different performance in case of wideband designs.

If the operating frequency f_0 is mapped onto the free parameter ξ generating the high-efficiency continuum in such a way that increasing f_0 corresponds to increasing ξ, which is the most common although not the only possible choice, class-F is characterized by non-Foster f_0 and Foster $2f_0$ load trajectories, whereas inverse class-F has the opposite trend. The theoretical waveforms and corresponding loading conditions for the two aforementioned cases are summarized in Fig. 1.

Although non-Foster trajectories cannot be synthesized with passive matching networks over broad bands, it is typically possible to approximate them by means of Foster trajectories when they have a resistive component. On the contrary, this is almost impossible when such non-Foster trajectories are purely reactive, i.e., on the border of the Smith chart. In the case of the inverse class-F PA, accurately tracking the $2f_0$ impedance trajectory is not possible with standard passive matching networks. Also, the required $3f_0$ load is

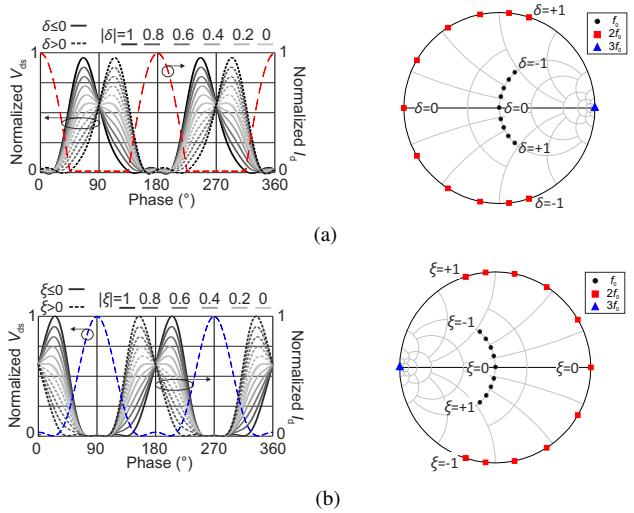

(a)

(b)

Fig. 1. Theoretical waveforms (left) and optimum loads (right) of the continuous (a) class-F and (b) inverse class-F.

a short circuit regardless of the value of the parameter ξ. Therefore, in this case, keeping the phase rotation limited helps in minimizing the mismatch at both harmonic frequencies.

III. Design and Fabrication

In this work, a continuous inverse class-F PA is designed to cover a frequency band of 600 MHz around 1.75 GHz.

One of the issues of harmonic tuning in wideband designs is related to the possible superposition of the highest frequency of the n-th harmonic range with the lowest frequency of the $(n+1)$-th, thus requiring a trade-off between operating frequency band and the achievement of the theoretical loading conditions [3]. The selected band (1.4-2 GHz) is the widest one allowing for a non-overlap of the $2f_0$ and $3f_0$ ranges while allowing for a sufficient distance between the f_0 and $2f_0$ ranges to avoid undesired resistive impedance components in the lower end of the $2f_0$ range.

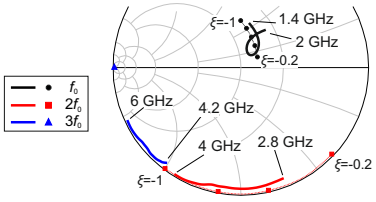

Fig. 2. Target (symbols) and synthesized (solid) load impedances at the current generator plane.

It was chosen to exploit only part of the design space of the continuous inverse class-F PA, namely $-1 \leq \xi \leq -0.2$, and to adopt a low-order output matching network (OMN) topology, in order to limit the phase rotation, especially at the harmonics, thus limiting the mismatch caused by the non-Foster $2f_0$ target trajectory. The OMN has been designed starting from a narrowband implementation at 1.75 GHz based on a three-section line-stub topology [6], where each line-stub block controls independently one of the harmonics. The OMN has then been optimized over the band of interest by minimizing the mismatch compared to the target impedance trajectories corresponding to $-1 \leq \xi \leq -0.2$. The synthesized loads at the current generator plane of the active device are compared to the target ones in Fig. 2. The matching at f_0 is at least 15 dB over the whole band, whereas the phase mismatch (in terms of reflection coefficients) at $2f_0$ and $3f_0$ is maintained within 50°. During the optimization phase, the OMN simplifies reducing to a two-stage line-stub topology.

The input matching network (IMN), which includes series and parallel frequency-selective stabilization elements to ensure stability in and out of band, is designed according to two requirements. In the f_0 range, minimum reflections are pursued thanks to conjugate matching, whereas, in the $2f_0$ range, the IMN has to present a reactive impedance providing the optimum trade-off between efficiency and AM/AM [7].

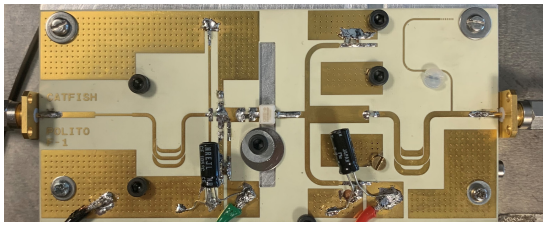

Fig. 3. Photograph of the inverse class-F PA prototype.

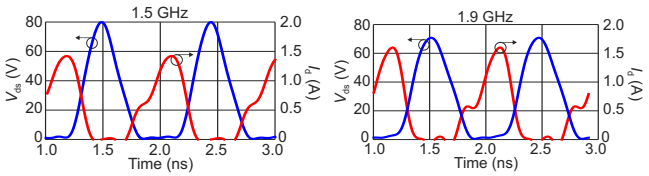

(a)

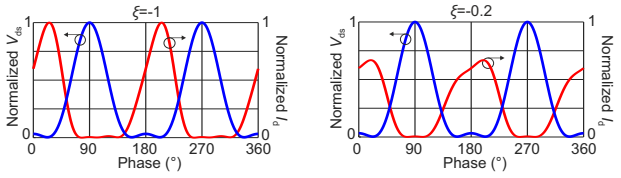

(b)

Fig. 4. Drain voltage (blue) and current (red) waveforms at the current generator plane, (a) simulated at 1.5 GHz and 1.9 GHz and (b) predicted by theory for $\xi = -1$ and $\xi = -0.2$.

The PA is manufactured on a Rogers 4350b substrate with 3.66 relative dielectric constant, 0.762 mm substrate thickness, and 35 μm metal thickness, and mounted on an aluminum carrier for heat dissipation. The photograph of the realized prototype is shown in Figure 3.

The simulated waveforms predicted by the device non-linear model at the current generator plane are shown in Fig. 4(a) at the frequencies of 1.5 GHz and 1.9 GHz, close to the band edges. As a reference, the theoretical waveforms corresponding to the extreme cases ($\xi = -1$ and $\xi = -0.2$) are shown in Fig. 4(b). The simulated results correctly reproduce the half-rectified sinusoidal voltage and the current waveforms

predicted by the theory, despite some slight discrepancy due to non-ideal harmonic loading conditions.

IV. Characterization Results

The PA is characterized in small and large signal conditions at the nominal bias $V_{DS} = 28\,V$, $V_{GS} = -2.72\,V$, corresponding to a quiescent drain current $I_D = 85\,mA$.

The small signal performance from 1 GHz to 3 GHz is reported in Fig. 5, where measured results (symbols) are compared to simulated ones (solid) showing very good agreement, with measured input and output return loss below 6 dB and 10 dB, respectively, and associated gain higher than 17 dB from 1.4 GHz to 2 GHz.

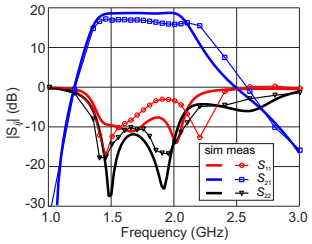

Fig. 5. Simulated (solid) and measured (symbols) scattering parameters of the inverse class-F PA.

The continuous wave (CW) large signal characterization is performed adopting a real-time vector test bench, calibrated using a 2-port Short-Open-Load-Thru (SOLT) routine, plus a SOL additional calibration at an extended port connected to a power meter for the absolute power calibration. The good agreement between measurements and simulations in the whole targeted band shown in Fig. 6, apart from a 50 MHz shift visible in the saturated efficiency performance and probably due to SMD components tolerances, proves the effectiveness of the design strategy. At the 3 dB gain compression point, the amplifier demonstrates output power, gain and efficiency in excess of 40 dBm, 13 dB and 70%, respectively. The presented hardware well compares with the state of the art (SOA), as evidenced by Table 1.

Two-tone measurements with 20 MHz tone spacing demonstrate a worst-case inter-modulation distortion (given by the high third-order inter-modulation product) power of -30 dBc around 1 dB gain compression, with associated efficiency of 55% at 1.75 GHz.

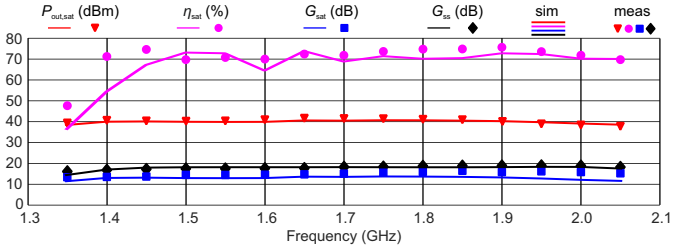

Fig. 6. Simulated (solid lines) and measured (symbols) CW performance of the inverse class-F PA.

Table 1. Comparison with SOA PAs at similar frequencies.

Device	Topology	Freq (GHz)	BW %	P_{out} (dBm)	η (%)	Gain (dB)	Ref.
bare die	F^{-1}	1.8–2.2	20	55.4	75	19	[2]
bare die	F^{-1}	2.6	–	35	78	14	[7]
packaged	Doherty	1.8–2.3	24	42	62	8	[8]
packaged	E_M/F_3	1.4–2	35	39.2	65	12	[9]
packaged	$\mathbf{F^{-1}}$	**1.4–2**	**35**	**40**	**70**	**13**	**T.W.**

V. Conclusion

A continuous inverse class-F PA designed for wideband operation to cover the 5G FR1 bands between 1.4 and 2 GHz, targeting base station applications, has been presented. The selection of the input and output terminations has been discussed, highlighting the main design choices. The fabricated demonstrator, based on a 10 W packaged Wolfspeed's device, shows at 3 dB gain compression an output power of 40 dBm, with corresponding efficiency and gain higher than 70% and 13 dB, respectively, over the frequency band 1.4-2 GHz. The linearity evaluated with 20 MHz-spaced two-tone measurements demonstrates inter-modulation products below -30 dBc around 1 dB gain compression, with associated efficiency of 55% at 1.75 GHz. The prototype performance is well in line with state-of-the-art PAs at these frequencies and is accurately predicted by simulations, proving the effectiveness of the design strategy.

References

[1] A. Piacibello, R. Quaglia, V. Camarchia, C. Ramella, and M. Pirola, "Dual-input driving strategies for performance enhancement of a Doherty power amplifier," in *2018 IEEE MTT-S International Wireless Symposium (IWS)*, 2018, pp. 1–4.

[2] T. Sharma, N. Zhu, J. Roberts, and D. H. Holmes, "Novel Continuous Inverse Class F Power Amplifier for High Power 5G Macro Base Station Application," in *2021 IEEE MTT-S International Microwave Symposium (IMS)*, 2021, pp. 729–731.

[3] M. Yang, J. Xia, Y. Guo, and A. Zhu, "Highly Efficient Broadband Continuous Inverse Class-F Power Amplifier Design Using Modified Elliptic Low-Pass Filtering Matching Network," *IEEE Trans. Microw. Theory Techn.*, vol. 64, no. 5, pp. 1515–1525, 2016.

[4] F. Raab, "Maximum efficiency and output of class-F power amplifiers," *IEEE Trans. Microw. Theory Techn.*, vol. 49, no. 6, pp. 1162–1166, 2001.

[5] Y. Y. Woo, Y. Yang, and B. Kim, "Analysis and experiments for high-efficiency class-F and inverse class-F power amplifiers," *IEEE Trans. Microw. Theory Techn.*, vol. 54, no. 5, pp. 1969–1974, 2006.

[6] A. Grebennikov, "Load network design technique for class F and inverse class F PAs," *High Frequency Electronics*, vol. 10, no. 5, pp. 58–72, 2011.

[7] T. Sharma, J. S. Roberts, S. K. Dhar, S. Shukla, R. Darraji, D. G. Holmes, and F. M. Ghannouchi, "On the Efficiency and AM/AM Flatness of Inverse Class-F Power Amplifiers," in *2019 IEEE MTT-S International Microwave Symposium (IMS)*, 2019, pp. 460–463.

[8] M. Yang, J. Xia, and A. Zhu, "A 1.8–2.3 GHz broadband Doherty power amplifier with a minimized impedance transformation ratio," in *2015 Asia-Pacific Microwave Conference (APMC)*, vol. 1, 2015, pp. 1–3.

[9] M. Safari Mugisho, M. Thian, A. Piacibello, V. Camarchia, and R. Quay, "Bandwidth and Power Back-Off Performances of a Class-E_M/F_3 Power Amplifier," in *2021 European Microwave Conference*, 2021.